New Method for Designing Shock-Free Transonic Configurations

H. Sobieczky,* N. J. Yu,† K-Y. Fung,‡ and A. R. Seebass§
University of Arizona, Tucson, Ariz.

A new method for the design of shock-free supercritical airfoils, wings, and three-dimensional configurations is described. Results illustrating this procedure in two and three dimensions are given. They include modifications to part of the upper surface of an NACA 64A410 airfoil that will maintain shock-free flow over a range of Mach numbers for a fixed lift coefficient, and the modifications required on part of the upper surface of a swept wing with an NACA 64A410 root section to achieve shock-free flow. While the results are given for inviscid flow, the same procedures can be employed iteratively with a boundary-layer calculation in order to achieve shock-free viscous designs. With a shock-free pressure field, the boundary-layer calculation will be reliable and not complicated by the difficulties of shock wave, boundary-layer interaction.

Introduction

WELL-KNOWN requirements for increased efficiency and, in the case of commercial aircraft, productivity have forced the operating conditions of compressors, turbines, propellers, wing sections, and aircraft into the transonic regime. Unfortunately, once local regions of supersonic flow occur, shock waves are likely with the attendant wave drag and boundary-layer separation losses. In the mid 1950s, Morawetz[1] proved that shock-free, two-dimensional, irrotational, near-sonic flows are mathematically isolated. In other words, any arbitrary¶ changes in the flow or boundary conditions that provide a shock-free flow will lead to the formation of a shock wave. Thus, Morawetz's theorem stated that the shock-free inviscid flow solutions, if and when they existed, were isolated by neighboring solutions that contain shock waves. Recently, this result has been extended to three dimensions by Cook.[2] Fortunately, it was recognized that such flow would have practical significance if, as seemed likely, the shock waves that occurred in neighboring flows were very weak. Wind tunnel research by Whitcomb[3] at the NASA Langley Research Center and Pearcey[4] at the National Physical Laboratory, United Kingdom, led to the development of practical "shock-free" airfoil sections. Subsequent analytical studies by Garabedian and Korn,[5] Nieuwland,[6] Boerstoel,[7] and Sobieczky[8] established theoretical design procedures for two-dimensional inviscid flows. More recently, the development of sophisticated numerical codes for the analysis of transonic flowfields has led to the design of both airfoils and wings by numerical optimization.[9,10] The practical success of the preceding efforts, as documented by the recent NASA Conference on Advanced Technology Research,[11] has been substantial. Further progress, as reported here, seems likely. The senior author recognized that the procedure he was using in the hodograph plane implied an analogous procedure in the physical plane, and furthermore, that this procedure did not seem to be restricted to two-dimensional flows.[12,13] This paper reports the success to date in using this idea to provide shock-free designs in two and three dimensions.

The design procedure invoked here is, in principle, a simple one. While there is no guarantee that a shock-free flow will necessarily result from the procedure, our experience in two dimensions has been that if the hodograph method will work for specified flow and airfoil parameters, then the procedure outlined here will work too. Also, it provides neighboring shock-free airfoil shapes for fixed lift coefficient with varying Mach numbers and varying lift coefficient for fixed Mach numbers, as well as providing a multiplicity of closely related shapes that are shock free at fixed lift coefficient and Mach number. This wealth of shock-free, two-dimensional designs is no great surprise; therefore, it is not surprising that they are found with minimal computational effort. Two-dimensional inviscid flow potential airfoil designs require less than a minute of CYBER 175 CPU time and only a few seconds of CDC 7600 CPU time.

For three-dimensional flows our results are less extensive. Also, while it is clear that the procedure we use rests on a sound mathematical foundation in two dimensions, this is not the case in three dimensions. Indeed, for three-dimensional (that is, nonplanar and nonaxisymmetric) flows we solve an ill-posed boundary value problem.** That this problem can be solved successfully is a result of the practical requirement for specifying chordwise modifications more densely than spanwise ones.

We have demonstrated the ability to modify three-dimensional wings so that, within the context of the numerical algorithm used, shock-free flows are obtained. We have not yet demonstrated an analogous wealth of shock-free flows in the three-dimensional case, but see no reason to believe that this situation is different there. The practical consequences of this wealth should prove to be of interest to the aircraft industry.[14] Its success will depend on the designer being able to choose baseline configurations that will result in good off-design performance and not compromise nonaerodynamic requirements.

Design Procedure

The procedure we use to find shock-free designs assumes that a reliable numerical code is available for computing the flow past a given configuration, such as that sketched in Fig.

**The authors are indebted to A. Jameson of the Courant Institute for alerting them to this difficulty.
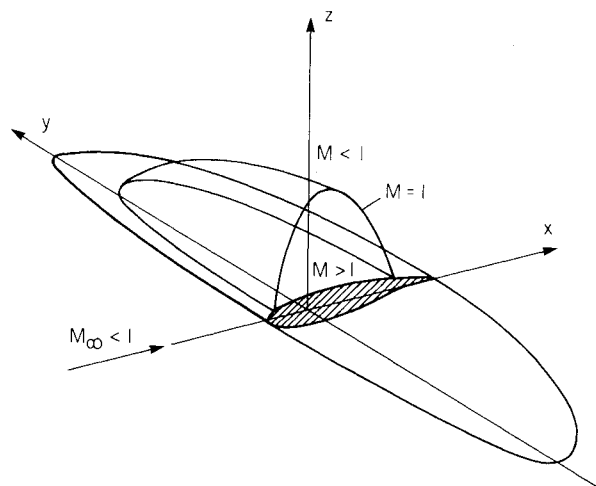
Fig. 1 Sketch of shock-free flow past a lifting wing depicting the sonic surface obtained by introducing fictitious behavior inside this surface that results in elliptic equations.

1. Such codes are available for two- and three-dimensional inviscid flows. When they are coupled with a reliable boundary-layer code, the design procedure outlined here can be used to calculate shock-free viscous flow designs. While this would require some modest iteration, it is certainly possible both in practice and in principle. With the existence of a reliable analysis algorithm presumed we modify this algorithm so that once the flow become hyperbolic we alter the basic equations so that they revert to elliptic behavior. This may be done in a number of ways, but it should be done in a way that it conserves new, but fictitious, "mass" and "momentum" fluxes to a satisfactory degree of accuracy. We may, for example, change the density's dependence from the usual one to one that returns the equations to elliptic form. We might suppose, for the purpose of illustration, that once the equations become parabolic (i.e., sonic) on some surface, then at higher velocities the density will be maintained at its sonic value, giving elliptic equations. We use a numerical algorithm to compute this fictitious flow past a configuration of interest, chosen perhaps on the basis of previous design experience. Because the equations are elliptic, this will result in a discretized, pseudoanalytic description of the velocity, density, and pressure fields on the embedded parabolic surfaces, and this description will be consistent with the correct governing equations. These initial data on the parabolic surfaces are then used to calculate the correct flowfield inside such surfaces. This new flowfield may or may not contain shock waves. This depends on the choice of the fictitious equations, or perhaps better, fictitious gas, used inside the parabolic surfaces. This new flow will define a stream surface that is tangent to, and has the same curvature as, the stream surface at the intersection of the sonic surface and the original body. Inside this surface a new body shape is defined by the stream surface of the new, but now real, flow.

Here, of course, we must also address the question of well-posedness. In two dimensions there is no difficulty because either of the spatial coordinates may be designated as the time-like variable. This is not the case in three dimensions where only the spatial coordinate aligned with the flow is time-like. Because shock-free flows are reversible, the domains of dependence and influence may be interchanged. But neither the normal (nor the binormal) to the stream direction can be considered time-like in the three-dimensional initial-value problem. Thus, data are given on surfaces that are not in the usual domain of dependence and the problem is ill-posed. It is this fact that has made us stress that a reliable analysis algorithm should be the basis for the design computations. An analysis of three-dimensional model problems shows that only

variations in the spanwise direction that are on scale, that is, small compared to the nominal axial (flow direction) distance, will amplify; thus, the success of the numerical algorithm depends upon not introducing such disturbances. This is not the first time ill-posed problems have been solved to obtain results of engineering interest (see, for example, Ref. 15, pp. 448-472).

Fictitious Gas

As just mentioned, modifications are made to the basic equations to retain their elliptic behavior once the flow has accelerated to sonic speed and a parabolic surface, with the needed initial data, has been generated. The possible modifications are manifold. Our discussion is limited to those used to obtain the results reported here.

For two-dimensional flows we have used Jameson's[16,17] circle-plane algorithm for the full potential equation. Thus, in the analysis mode, we are solving

$$\{\rho\phi_x\}_x + \{\rho\phi_z\}_z = 0 \tag{1a}$$

with

$$\rho/\rho_\infty = \left[1 + \frac{\gamma-1}{2} M_\infty^2 (1 - \phi_x^2 - \phi_z^2) \right]^{1/\gamma - 1} \tag{1b}$$

where ϕ is the velocity potential and ρ the density. If we limit our consideration to fictitious gases for which the density is a function of the square of the velocity, viz., $\rho = \rho(q^2)$, where $q^2 = U^2[\phi_x^2 + \phi_z^2]$, then gas laws of the form

$$\rho/\rho_* = (a_*/q)^P \qquad P < 1 \quad \text{for} \quad q > a_* \tag{1c}$$

will insure elliptic behavior; $P = 1$ gives parabolic behavior and the fictitious and real gases have the same value of $(d\rho/dq)_*$. An alternative choice, and the one used most extensively here, is $P = 0$; in this case, Eq. (1a) becomes Laplace's equation. When the flow would normally be hyperbolic, Eq. (1a) is now solved with the density-velocity relationship of Eq. (1c). A fictitious mass flow, which matches the real mass flux at the sonic surface, is thereby conserved and the velocity field remains irrotational.

For three-dimensional flows we have used the Ballhaus-Bailey-Frick algorithm,[18] as implemented by Mason et al.[19] This is a small perturbation calculation, and the classical conservative formulation is adopted here. Thus, in an equivalent form, we solve the system

$$-\tfrac{1}{2}(\gamma + 1)\{u^2\}_x + v_y + w_z = 0 \tag{2a}$$

$$v_z - w_y = 0 \tag{2b}$$

$$u_z - w_x = 0 \tag{2c}$$

where the velocity vector is $q = a_*[(1 + u)i + vj + wk]$.

A simple modification, Eq. (2), is to replace $\{u^2\}_x$ by $-\text{sgn}(u)\{u^2\}_x$ for all u. This system is elliptic, except on the sonic surface where $u = 0$. We may think of the first of Eqs. (2) as being the consequence of the small perturbation expansion for the density, viz.,

$$\frac{\rho}{\rho_*} - 1 = -u - \frac{\gamma-1}{2} u^2 \tag{3}$$

whereas the fictitious equation, with u replaced by $-|u|$ for $u > 0$, results from

$$\frac{\rho}{\rho_*} - 1 = -u + \frac{\gamma+3}{2} u^2 \tag{4}$$

This fictitious gas has the same value for $(d\rho/du)_*$ as the real gas, Eq. (3). For three-dimensional design studies, then, we

solve Eqs. (2) with $\{u^2\}_x$ replaced by $-\text{sgn}(u)\{u^2\}_x$; this corresponds to using the densities given by Eqs. (3) and (4) for $u < 0$ and $u > 0$, respectively.

Calculation of the Hyperbolic Flowfield

As previously described, we calculate the flow past a body using the correct equations when the flow is subsonic and a modified, incorrect, set of equations when the flow is supersonic. This calculation serves to define sonic surfaces on which the flowfield calculation is switched from the correct equations to the modified ones. Outside this surface, presuming the trailing edge of the wing is subsonic, the solution satisfies the correct equations, and the potential at infinity has the correct value for the circulation. If infinity in the physical plane is not mapped to a finite part of the computational plane, then there is, in principle, a need to correct the doublet and nonlinear contributions; in practice, these contributions are small and changes in them negligible. Thus, the flow in the elliptic, subsonic domains is fixed and known, as are the initial data we need on the parabolic surface.

For two-dimensional flows, the calculation of the correct hyperbolic behavior is carried out using the method of characteristics. This is done in a hodograph-like working plane in which the characteristics are orthogonal straight lines. If we take $\xi = \theta + \nu$ and $\eta = \theta - \nu$, where θ is the flow deflection angle and ν the Prandtl-Meyer turning angle, then the velocity potential and stream function satisfy

$$\phi_\xi = K\left(\frac{\xi-\eta}{2}\right)\psi_\xi, \quad \phi_\eta = -K\left(\frac{\xi-\eta}{2}\right)\psi_\eta \tag{5}$$

or, equivalently,

$$\left.\frac{d\psi}{d\phi}\right|_{\xi,\eta=\text{const}} = \pm K^{-1}$$

where the $\pm$ signs refer to $\xi, \eta = \text{const}$, respectively. Here

$$K(\nu) = K[\nu(q)] = \{|M^2(q) - 1|\}^{1/2}\rho(0)/\rho(q)$$

Values for the velocity potential on the parabolic line, $z = z^*(x)$, and the shape of this line are used along with the usual relations between the spatial coordinates and ϕ and ψ to find ψ on the sonic line. These initial data are then integrated using Eqs. (5) to determine the locus $\psi(x,z) = 0$ which passes through the intersection of the sonic line with the body sur-

face. The values of z for which $\psi(x,z) = 0$ determine the new body shape. This shape will have the same slope and, at least theoretically, the same curvature, as the original body at the sonic points. This follows from the observation that flow quantities are not changed at the sonic line; thus, the streamwise momentum and normal pressure gradient are unchanged. Consequently, the local flow curvature must be the same.

For three-dimensional flows, the calculation of the hyperbolic flowfield is carried out by a procedure that marches inward from the sonic surface by successive surfaces of constant density (isopycnics) for the full potential equation, or constant axial flow speed u for the small perturbation equation. We limit our discussion to the small perturbation equations, as all the results reported here are derived from them. Preliminary results using the full potential equations have been obtained by N. J. Yu.

We may either write Eqs. (2) in the appropriately scaled form or work with them directly as we will do here.

We are given an isotach surface $z^*(x,y)$, as shown in Fig. 2, on which we know $u = u^* = \text{const}$, $w = w^*(x,y)$, and $v = v^*(x,y)$. We use the data on this surface, and the surface shape, to calculate

$$z_x^*, \quad z_y^*, \quad w_x^*, \quad w_y^*, \quad v_x^*, \quad v_y^* \tag{6}$$

Because these data satisfy Eqs. (2), we can verify that

$$v_x^* = z_x^* w_y^* - z_y^* w_x^*$$

which can be used, if needed, to check the consistency of the initial data. The values given in Eq. (6) can now be used to calculate the z derivatives of u, w, v on $z^*(x,y)$, where $u(x,y,z^*) = \text{const}$, by using

$$u_z = [z_y^* v_x^* - z_x^* v_y^* - w_x^*]/J \tag{7a}$$

$$w_z = [(\gamma + 1)u^* z_x^* w_x^* - z_y^* w_y^* + v_y^*]/J \tag{7b}$$

$$v_z = [(\gamma + 1)u^* z_x^* v_x^* - w_y^* - z_y^* v_y^*]/J \tag{7c}$$

where J, the Jacobian, $\partial(u,v,w)/\partial(x,y,z)$, is:

$$J = (\gamma + 1)u^* z_x^{*2} - z_y^{*2} - 1$$

When the Jacobian, which is initially negative, vanishes, we can no longer compute the z derivatives; this corresponds to the subsequent formation of multivalued solutions, i.e., limit surfaces. If $J = 0$ occurs before the calculations produce a suitable stream surface defined by $w(x,y,0)$, $v(x,y,0)$, then they must be rejected.

With Eq. (7a) inverted to give $(dz/du)_*$, we take a set increment in u, Δu, to form a new isotach surface $z^*(x,y) + \Delta z^*(x,y)$. This new shape, along with the mean value of u between the two surfaces and the second and third of Eqs. (7), provides the new values, $w^*(x,y) + \Delta w^*(x,y)$, $v^*(x,y) + \Delta v^*(x,y)$, of w^* and v^* on the next isotach. These values and the shape of the subsequent isotach are then converted to continuous functions by one-dimensional cubic splines in the x and y coordinates. This "onion-peel"-like process is then continued until $z = 0$, unless a limit surface intervenes. In the latter event, the solution must be rejected. A more detailed discussion of this procedure is given in Ref. 20.

Two-Dimensional Results

We have explored rather extensively some of the modifications that can be made to an existing airfoil, namely, an NACA 64A410 airfoil, to obtain shock-free flow. We will call this the baseline airfoil; the airfoil shapes we generate are identical with this airfoil over that portion wetted by subsonic
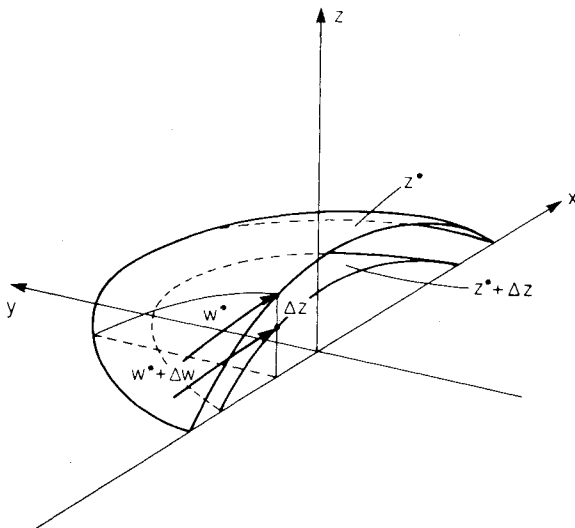

Fig. 2 Sketch of two neighboring isotach surfaces used in the calculation of the supersonic domain for Eqs. (2).

MACH = .720 ALPHA = 0.40

DESIGN (+) ORIGINAL (⊙)

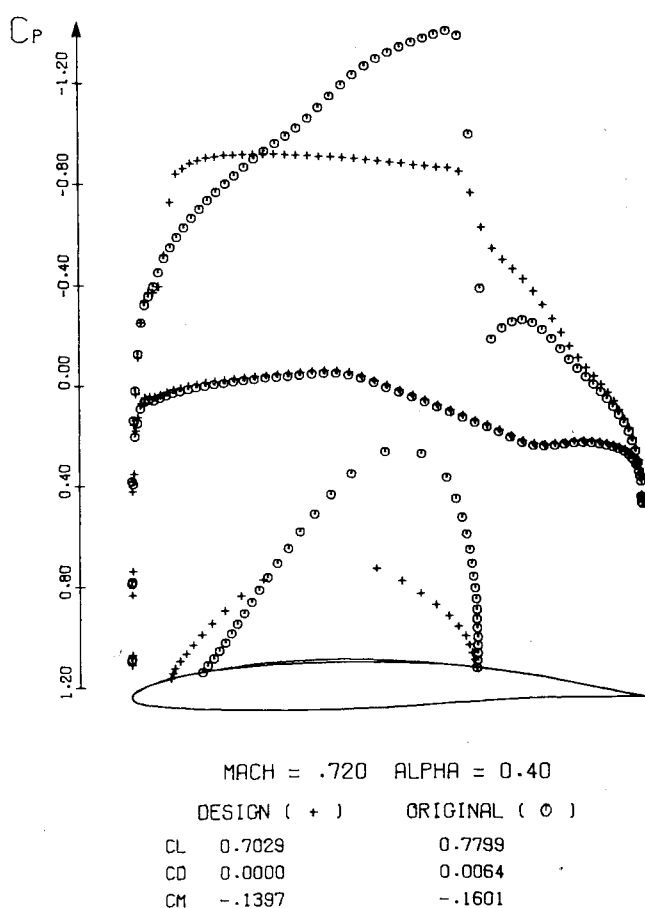|		
CL	0.7029	0.7799
CD	0.0000	0.0064
CM	-.1397	-.1601

Fig. 3 Comparison of the pressure coefficients and sonic lines for the baseline NACA 64A410 and the shock-free airfoil obtained from it by the direct design procedure.
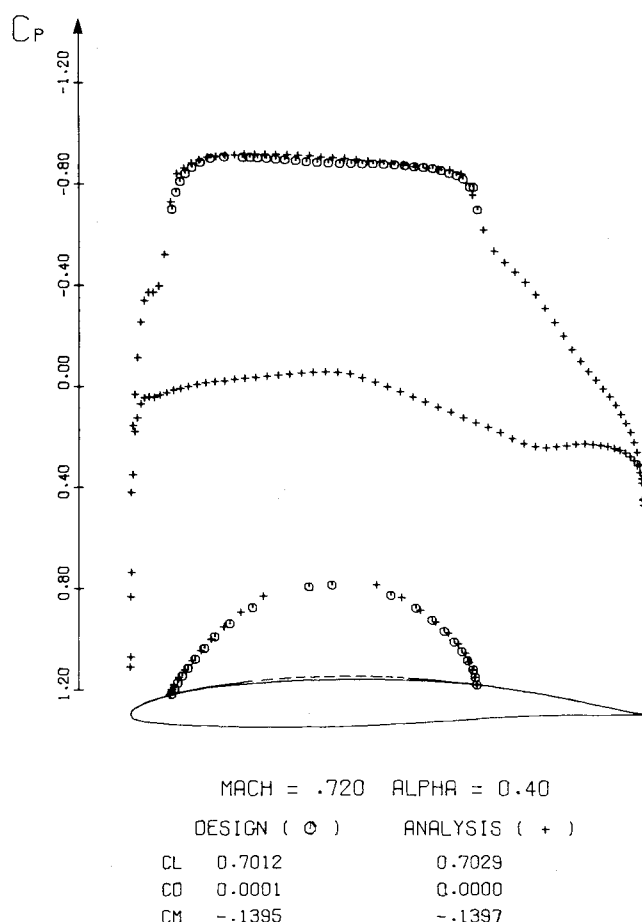

MACH = .720 ALPHA = 0.40

DESIGN (⊙) ANALYSIS (+)

CL	0.7012	0.7029
CD	0.0001	0.0000
CM	-.1395	-.1397

Fig. 5 Comparison of the pressure coefficient and the sonic line obtained by the design calculation that modifies the airfoil shape with those obtained by computing the flow past the modified airfoil.

Fig. 4 Parameter space explored for the shock-free airfoils that can be obtained when the baseline configuration is an NACA 64A410 airfoil.

flow; we need only modify the airfoil over a limited portion of its upper surface to obtain shock-free flows. Further, this modification is not unique for fixed flight conditions; rather, if one such shape exists, there usually will be a family of modifications of the baseline airfoil that will produce shock-free flow corresponding to different gas laws. Modifications to NACA 0012 and 64A410 airfoils that resulted in shock-free flows were reported by Eberle in Ref. 21.

With a baseline airfoil selected here mainly for illustrative purposes, we then pick a set of flight conditions for which we wish to find a modification of the airfoil shape that will result in shock-free flow. We choose $M_\infty = 0.72$ and the angle of attack $\alpha = 0.4$ deg. At these conditions inviscid flow calculations for the NACA 64A410 baseline airfoil give a C_L

of 0.78 and a C_D of 0.0064. The design procedure discussed earlier results in an airfoil that is 9.3% thick with a lift coefficient of 0.703. The original and design pressure coefficient, sonic lines and body shapes are compared in Fig. 3a; these results and all other "analysis" results were computed using the numerical algorithm of Ref. 16. Figure 3b compares the pressure coefficients and sonic lines determined by the design procedure with those computed for the design airfoil shape.

With this shock-free design established at $M = 0.72$ and with $C_L = 0.70$, we now wish to determine the families of shapes that provide shock-free flow for a fixed lift coefficient as the Mach number varies, and a fixed Mach number as the lift coefficient varies. This has been done with $P = 0$; that is, with a constant density fictitious gas (at the critical value), requiring an iterative procedure for the case at fixed lift coefficient. Other shapes were then explored that will produce the same lift coefficient, 0.70, at a fixed Mach number by taking P to be -0.5, 0.5, and 1.0. Also, for $P = 0$ we have determined the maximum Mach number for which the design procedure will produce a shock-free airfoil as a function of lift coefficient. This Mach number is nearly a linear function of lift coefficient at larger lift coefficients. The slope of this variation is consistent with that given by Boerstoel.[22] Preliminary studies also indicate that for a fixed lift coefficient of 0.6-0.7, an 0.1% increase in the maximum Mach number requires about an 0.2% reduction in the thickness for shock-free flow when the nominal thickness is about 10%. This result is less optimistic than the envelope of the hodograph designs given by Boerstoel,[22] who found that only an 0.1% reduction was required. In our study the generic family of the airfoil is invariant; we have not yet examined the
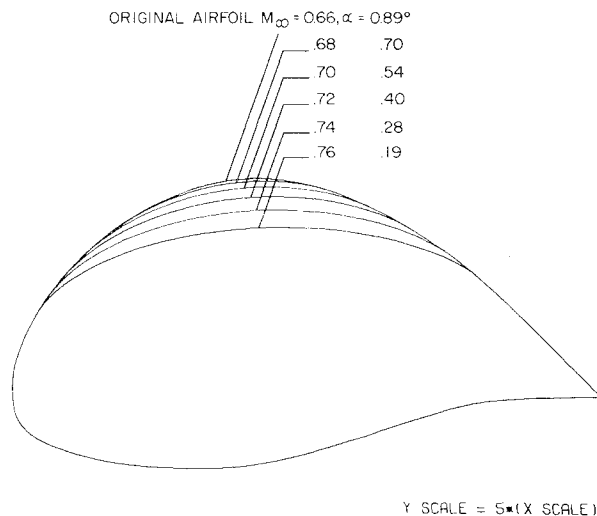
Fig. 6   Shock-free airfoil shapes for fixed lift coefficient $C_L = 0.70$ and varying Mach number. The fictitious gas has a constant density in the supersonic domain ($P = 0$). The baseline airfoil is an NACA 64A410.
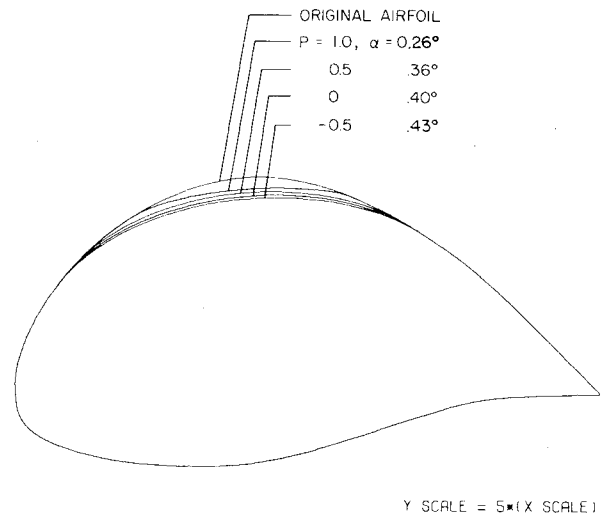

Fig. 8   Shock-free airfoils for fixed Mach number $M_\infty = 0.72$ and lift coefficient $C_L = 0.70$, varying the exponent P of Eq. (1c) and thus changing the density's dependence on flow speed. The baseline airfoil is an NACA 64A410.
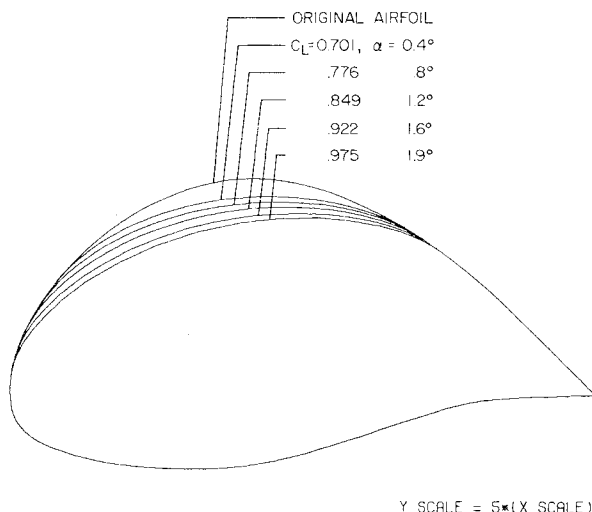

Fig. 7   Shock-free airfoil shapes for fixed Mach number $M_\infty = 0.72$ and varying lift coefficient. The fictitious gas has a constant density in the supersonic domain ($P = 0$). The baseline airfoil is an NACA 64A410.

modifications required when the baseline airfoil is near the envelope of hodograph designs. Positive values of P provide less airfoil thickness reduction, since the fictitious and real-gas densities are more nearly the same. The range of our airfoil studies is depicted in Fig. 4, with shock-free airfoils being determined for the points indicated. Also shown in Fig. 4 is the maximum Mach number for which a design was found as a function of lift coefficient for $P = 0$.

The accuracy of the design procedure was studied at a number of design points by comparing the design's pressure distribution and sonic line shape with those obtained using the unmodified numerical algorithm to analyze the design airfoil shape. Typical results are shown in Fig. 5. The sonic line shape and initial data on the sonic line are determined in the circle-plane; then they are mapped back to the physical plane. The method of characteristics in the hodograph variables is used to compute the design pressure coefficient corresponding to the calculated airfoil surface shape. The agreement, as shown, is excellent. For designs that approach the Mach number at which a limit line first penetrates the surface, special care must be taken with the analysis code in order to

obtain a converged solution. These designs have very rapid expansions immediately following the sonic line. Indeed, as Boerstoel[22] has noted, the analysis code used with an optimization scheme will not produce designs of this character.

The shock-free airfoil shapes that are obtained for fixed C_L and P, fixed M_∞ and P, and fixed M_∞ and C_L at various Ps, are shown in Figs. 6-8. One can overlay the results for fixed C_L and find quite similar airfoil shapes that are shock-free over a range of Mach numbers. Because modifications to the baseline airfoil are required only over a limited portion of the upper surface, and a family of specified changes in the airfoil curvature is known for each set of flight conditions, a closely related family of shock-free airfoil shapes can be generated. Thus, the minor modifications to a limited portion of a wing surface needed to produce shock-free flow over a practical range of flight conditions can be easily determined.

Three-Dimensional Results

Our first design results using the method just described were for two-dimensional, small perturbation flow past a parabolic arc airfoil. Consequently, we initiated our three-dimensional studies with a rectangular, unswept wing having an aspect ratio of six and a parabolic arc airfoil. We utilized the small perturbation approximation, Eqs. (2), and a parabolic thickness distribution; the airfoil was taken to be 6% thick at the centerplane. The flow was calculated using the algorithm of Ref. 19, modified to return the equations to elliptic behavior as described earlier. The initial data on the embedded sonic surface were then used to compute the correct flow in the supersonic domain using the "onion-peel" algorithm of Ref. 20. This defines new wing surface slopes. The flow past this shock-free design was then analyzed using the modified numerical algorithm. Figure 9 compares the pressure distributions on the original and design wing at various lateral positions for $M_\infty = 0.87$. Also shown are the cross sections of the sonic surface at the same lateral stations. The only essential differences in the pressure occur in the supersonic domain, which is consistent with the design process. The modifications made to the wing slope, shown in Fig. 10 for several lateral stations, have eliminated the shock wave.

A subsequent, more realistic, calculation was made for the planform sketched in Fig. 11. The wing section chosen was an NACA 64A410 profile at the center section and an elliptic thickness distribution. The leading-edge sweep was taken to be 30 deg, the trailing edge 15 deg, and the span-to-chord

Fig. 9 Sonic surface for the shock-free rectangular wing obtained by modifying a wing with a parabolic arc airfoil section and the pressure coefficients on the original and modified wing, as calculated by the numerical algorithm of Ref. 19. The thickness distribution of the baseline wing is parabolic in y/c.
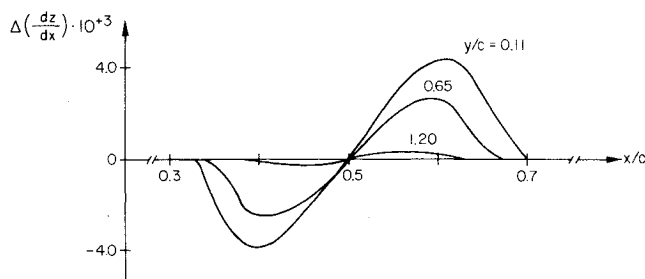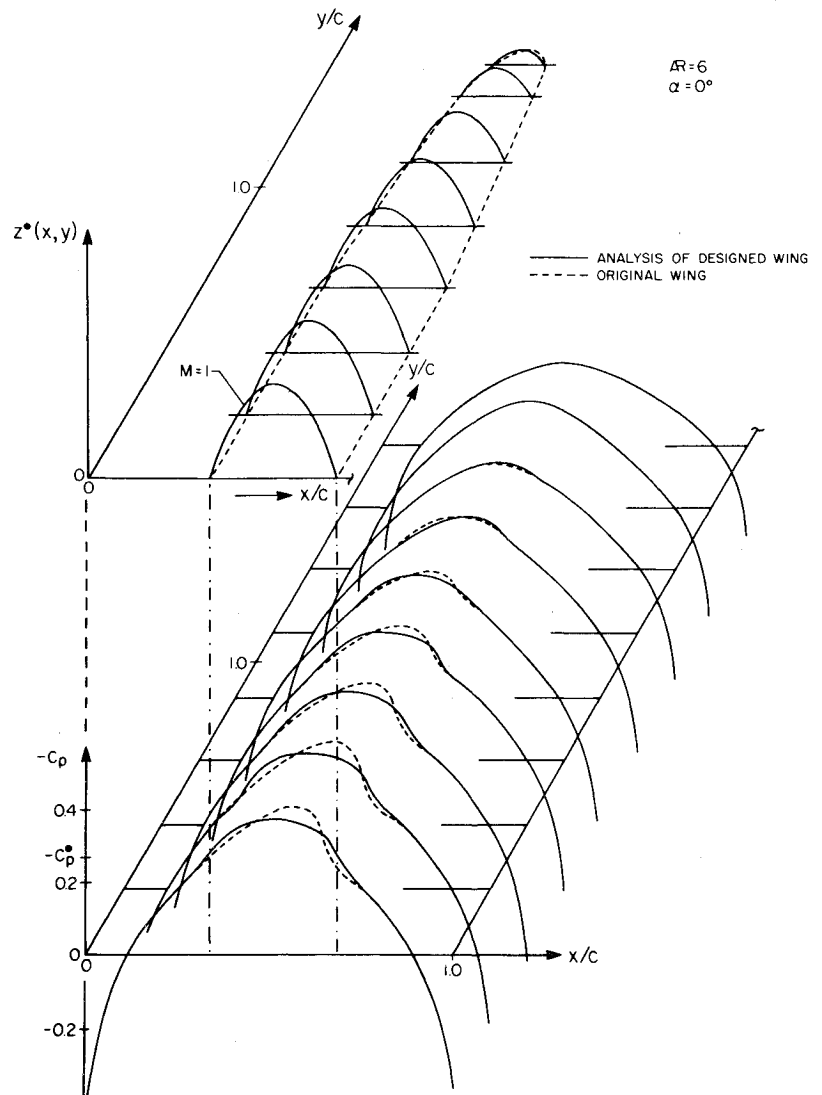

Fig. 10 Changes required in the surface slope at various lateral stations to provide shock-free flow over the rectangular wing of Fig. 9.

ratio was 5. The sonic surface is also depicted in Fig. 11. Figure 12 compares the pressure coefficients on the upper surface of the original wing and the wing designed to be shock free. While the reduction in drag for this wing is small compared to the induced drag, it is clear that the wing modifications have essentially eliminated the shock waves, and, consequently, the wave drag. More importantly, shock wave induced boundary-layer separation is avoided. Impressive results for the ONERA M6 planform have been obtained by Yu[23] using the full potential equation.

At this point we stress that the preceding comparison is obtained by computing the flow past the original wing and the design wing using the same numerical algorithm. The process

that leads to the new wing shape also provides the pressure on the wing.

Conclusion

A novel and simple procedure for determining modifications that will make a baseline configuration shock-free for supercritical flight conditions has been delineated. For two-dimensional, inviscid flows, shock-free designs are obtained in seconds on a CYBER 175. Families of airfoils that are shock free at fixed, as well as varying, flight conditions are found. The same procedure has been applied to three-dimensional wings, resulting in wing modifications that make the wings shock-free when the flow is analyzed with the numerical algorithm that was modified to become a design tool. It can also be applied to the design of shock-free cascades. A unique feature of the procedure is that any code that is effective in computing the flowfield may be modified in various ways to be a design algorithm, if it is coupled with a method for calculating the solution in the supersonic domains for given data on the sonic surfaces. A straightforward marching technique for such computations is described for three-dimensional flows; in two dimensions, either the marching procedure or the method of characteristics may be used for the supersonic domain. The algorithm for the supersonic domain serves to define the modifications needed in the configuration to achieve shock-free flow; these modifications will be limited to that portion of the design shape that are wetted by supersonic flow.
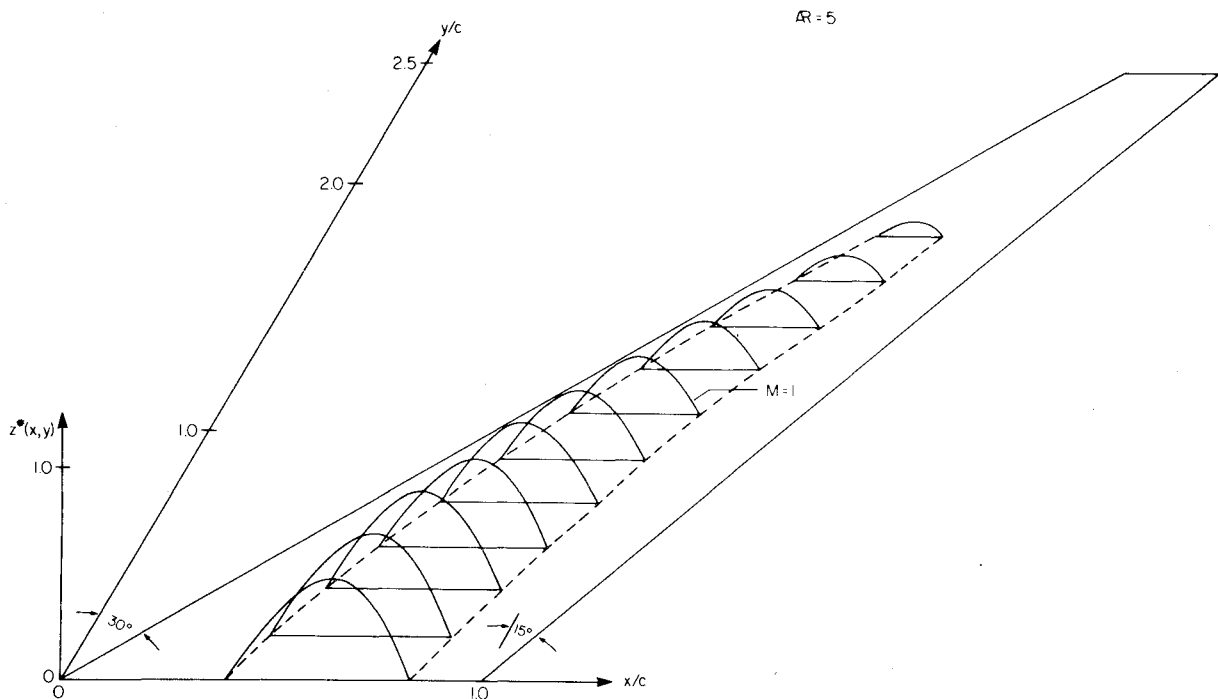
Fig. 11   Sonic surface on the shock-free swept wing designed from a wing with an NACA 64A410 center section profile and an elliptic thickness distribution. The leading edge sweep is 30 deg; the trailing edge sweep 15 deg.
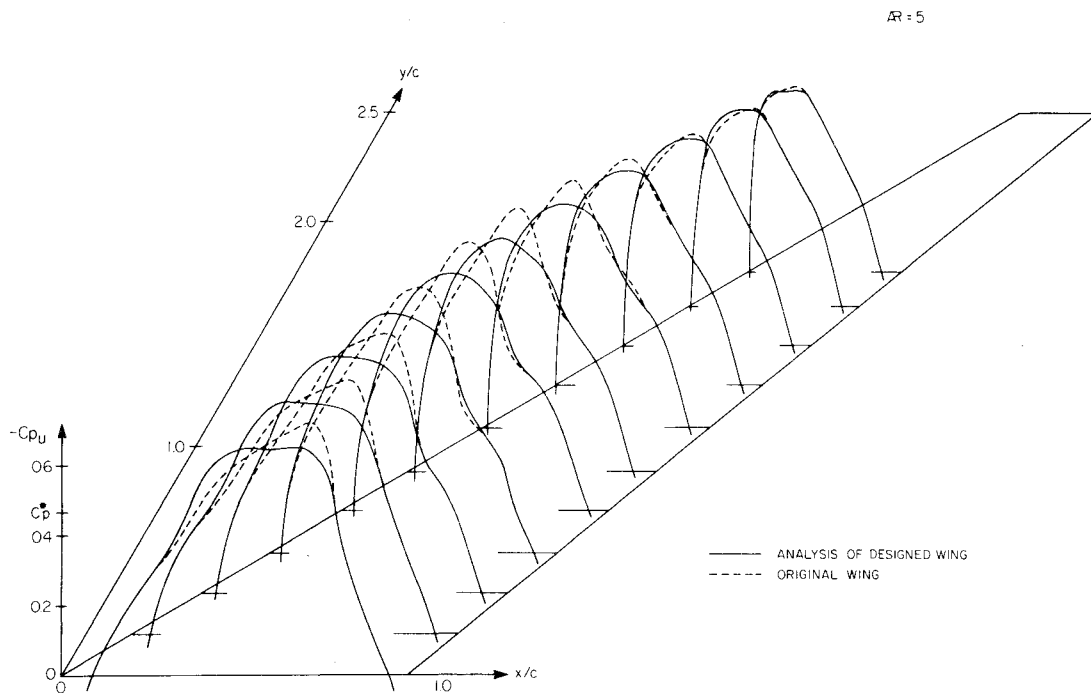

Fig. 12   Comparison of the computed pressure coeffcient on the wing of Fig. 11 with an NACA 64A410 center section profile and an elliptic thickness distribution, with the pressure coefficient obtained by computing the flow past the modified wing using the same numerical algorithm.

Acknowledgment

References

[1] Morawetz, C. S., "On the Non-Existence of Continuous Transonic Flows Past Profiles, I, II, and III," *Communications on Pure and Applied Mathematics*, Vols. 9, 10, and 11, 1956, 1957, and 1958, pp. 45-68, 107-131, and 129-144.

[2]Cook, L. P., "A Uniqueness Proof for a Transonic Flow Problem," *Indiana University Mathematical Journal*, Vol. 27, Jan.-Feb. 1977, pp. 51-72.

[3]Whitcomb, R. T. and Clark, L. R., "An Airfoil Shape for Efficient Flight at Supercritical Mach Numbers," NASA TM X-1109 (confidential report), July 1965.

[4]Pearcey, H. H., "The Aerodynamic Design of Section Shapes for Swept Wings," *Advances in Aeronautical Sciences*, Vol. 3, 1962, pp. 277-322.

[5]Garabedian, P. R. and Korn, D. G., "Numerical Design of Transonic Airfoils," *Numerical Solution to Partial Differential Equations*, Vol. II, Academic Press, New York, 1978, pp. 253-271.

[6]Nieuwland, G. Y., "Transonic Potential Flow Around a Family of Quasi-Elliptical Airfoil Sections," Nationaal Lucht-en Ruimtevaart Laboratorium Rept. TR-T 172, Amsterdam, The Netherlands, 1967.

[7]Boerstoel, J. W., "Design and Analysis of a Hodograph Method for the Calculation of Supercritical Shock-Free Airfoils," Nationaal Lucht-en Ruimtevaart Laboratorium Rept. TR 77046 U, Amsterdam, The Netherlands, 1977; also Boerstoel, J. W, and Huizing, G. H., "Transonic Shock-Free Aerofoil Design by an Analytic Hodograph Method," AIAA Paper 74-539, Palo Alto, Calif., June 1974.

[8]Sobieczky, H., "Entwurf überkritischer Profile mit Hilfe der rheoelektrischen Analogie," Deutsche Forschungs-und Versuchsanstalt für Luft-und Raumfahrt Rept. DLR-FB 75-43, Göttingen, West Germany, 1975.

[9]Hicks, R. M. and Vanderplaats, G. N., "Application of Numerical Optimization to the Design of Supercritical Airfoils Without Drag-Creep," SAE Paper 770440, Business Aircraft Meeting, 1977.

[10]Hicks, R. and Henne, P. A., "Wing Design by Numerical Optimization," AIAA Paper 77-1247, Seattle, Wash., Aug. 1977.

[11]*Advanced Technology Airfoil Research*, Proceedings ATAR Conference, NASA Langley Research Center, March 1978.

[12]Sobieczky, H., "Die Berechnung lokaler Räumlicher Überschallfelder," lecture at Gesellschaft für angewandte Mathematik und Mechanik, Copenhagen, May-June 1977, *ZAMM* 58T, 1978, pp. 215-216.

[13]Sobieczky, H., "Transformation Methods for Three-Dimensional Compressible Flow," Deutsche Forschungs-und Versuchsanstalt für Luft-und Raumfahrt Rept., Göttingen, West Germany, in preparation.

[14]Sobieczky, H. and Seebass, A. R., "Adaptive Airfoils and Wings for Shock-Free Supercritical Flight," Invention Disclosure, University of Arizona, Tucson, Ariz., May 1978.

[15]Hayes, W. D. and Probstein, R. F., *Hypersonic Flow Theory, Vol. I, Inviscid Flows*, Academic Press, New York, 1966.

[16]Jameson, A., "Iterative Solution of Transonic Flows Over Airfoils and Wings," *Communications on Pure and Applied Mathematics*, Vol. 27, 1974, pp. 283-309.

[17]Bauer, F., Garabedian, P., Korn, D., and Jameson, A., "Supercritical Wing Sections," *Lecture Notes in Economics and Mathematical Systems*, M. Beckmann and H. P. Kunzi (Eds.), Vol. 108, Springer-Verlag, Berlin, Heidelberg, New York, 1975.

[18]Ballhaus, W. F., Bailey, F. R., and Frick, J., "Improved Computational Treatement of Transonic Flow about Swept Wings," *Advances in Engineering Sciences*, NASA CP-2001, 1976.

[19]Mason, W. H., Mackenzie, D., Stern, M., Ballhaus, W. F., and Frick, J., "An Automated Procedure for Computing the Three-Dimensional Transonic Flow over Wing-Body Combinations, Including Viscous Effects," Vols. I and II, Air Force Flight Dynamic Laboratory Rept. AFFDL-TR-77, Wright-Patterson AFB, Ohio, Feb. 1978.

[20]Sobieczky, H., "A Computational Algorithm for Embedded Supersonic Flow Domains," University of Arizona Engineering Experiment Station Rept., Tucson, Ariz., July 1978.

[21]Eberle, A., "Profiloptimierung für transsonische Strömung mittels der Methoden der finiten Elemente und Charakteristiken," *MBB Report* UFE 1362 (0), 1977.

[22]Boerstoel, J. W., "Review of the Application of Hodograph Theory to Transonic Airfoil Design and Theoretical and Experimental Analysis of Shock-Free Airfoils," *Symposium Transsonicum II*, K. Oswatitsch and D. Rues (Eds.), Springer-Verlag, Berlin, Heidelberg, New York, 1976, pp. 109-133.

[23]Yu, N. J., "An Efficient Transonic Shock-Free Wing Redesign Procedure Using a Fictitious Gas Method," AIAA Paper 79-0075, New Orleans, La., Jan. 1979.